

## Influence of Welding Parameters on the Fatigue Behaviours of Friction Stir Welds of 3003-O Aluminum Alloys

Hakan AYDIN<sup>1\*</sup>, Ali BAYRAM<sup>1</sup>, M. Tahir YILDIRIM<sup>2</sup>, Kurtuluş YIĞIT<sup>1</sup>

<sup>1</sup> Uludağ University, Faculty of Engineering and Architecture, Department of Mechanical Engineering, 16059, Görükle-Bursa, Turkey

<sup>2</sup> Mako Electricity Industry and Commercial Corporation, 16159, Nilüfer-Bursa, Turkey

Received 25 June 2010; accepted 03 November 2010

Friction stir welding is a solid state welding method which appeared as a relatively new welding technology to be used mostly in aluminum alloys. The fatigue behaviours of welded joints represents the main problem for their industrial applications. In this research, fully reversed uniaxial fatigue tests have been performed in order to investigate the fatigue behaviours of single-sided friction stir butt welds in different welding conditions in 3 mm thick 3003-O non-heat-treatable aluminum alloys. The employed rotating speeds of the tool were 1070, 1520 and 2140 rpm while the welding speeds were 40, 80 and 112 mm/min. The microstructure of the friction stir welds was studied by employing optical microscopy. The friction stir welds consisted of following microstructures: stirred zone, thermo-mechanically affected zone, heat affected zone and base material. The comparative studies on the fatigue behaviours between the base material and friction stir welds in different welding conditions have been done in this study. The fracture surfaces of the fatigue specimens were observed with a scanning electron microscope. According to the results, welding parameters have a major influence on the fatigue behaviours of the 3003-O friction stir welds. The fatigue lifes of FS welds with the welding speed of 40 mm/min at different rotating speeds are about 2–3 times longer than those of FS welds with the welding speeds of 80 mm/min and 112 mm/min at different rotating speeds at a fixed stress amplitude under the stress ratio  $R = -1$ . At a significantly lower welding speed and a higher rotational speed the fatigue life of the friction stir welds of 3003-O aluminum alloys was improved due to the increased amount of heat supplied to the weld per unit length. However, the fatigue lifes of all friction stir welds are lower than that of the base material at all stress amplitudes.

*Keywords:* friction stir welding, welding speed, rotating speed, 3003 aluminum alloy, fatigue behaviour, fracture surface.

### INTRODUCTION

Aluminum alloys find a wide variety of applications in many important manufacturing areas, such as the automobile industry, aeronautics and the military because of its remarkable combination of characteristics, such as good strength to weight ratio, high corrosion resistance, easy workability and high electrical and heat conductivity [1–3]. The increasing relevance of aluminium alloys in industry requires research on more efficient and reliable joining processes [4]. In industry the aluminium alloys welding is the most often performed in pure argon shield by GTA or MIG methods [5]. However, conventional welding methods, when applied to aluminum alloys, present a series of disadvantages that have sometimes discouraged the use of such kinds of welded materials [2]. In recent years new welding technologies have appeared such as friction stir welding (FSW). FSW is a solid state welding method developed and patented by TWI in the 1991 [6], and now being increasingly used in the welding of aluminum alloys for which fusion welding is often difficult [7, 8]. One of the main advantages of FSW method compared to conventional fusion welding processes is the improvement of fatigue strength [9,10]. In addition, since the material subjected to FSW does not melt and recast, the resultant joint offers several advantages over traditional fusion welds such as less distortion, lower residual stresses and fewer weld defects [7]. FSW expands the capabilities of welding light alloys

such as aluminium, magnesium, titanium and their composites [9]. Application ranges from the production of small-scale components, such as cooling elements and electric engines, to welding of large panels, e.g. in ship building, in train wagons and trams, in offshore structures, and in bridge constructions [11].

FSW uses a rotating and traversing nonconsumable tool to generate frictional heat and cause mechanical deformation at the joint [12–14]. During FSW, the rotating tool induces a complex deformation in the surrounding material that varies depending on the joining materials and welding conditions [7]. The heat of friction and plastic flow arising from the rotating tool produce significant microstructural changes, which lead to a local variation in the mechanical properties of the weld [2, 3, 8, 14–17]. This flow strongly depends on the welding parameters and tilt angle [9]. The FSW weld zone consists of a stirred zone, a thermomechanically affected zone (TMAZ) and a heat-affected zone (HAZ) [8, 9, 14]. The FSW process results in obtaining a very fine and equiaxed grain structure in the stirred zone giving a higher mechanical strength and ductility [8, 14, 18–20]. Cavaliere and Panella [9] also reported that the fine grain size of the stirred zone and the solid state transformations acting in the TMAZ and HAZ lead to high tensile strength and enhanced fatigue properties with respect to traditional fusion techniques.

Fatigue is one of the main causes of failure of welded structures, therefore many efforts have been done to investigate the fatigue properties of FSWed aluminum alloy joints [2, 5, 7, 9–12, 18, 21]. However, up to now the

\*Corresponding author. Tel.: +90-224-2940652; fax: +90-224-2941903.  
E-mail address: hakanay@uludag.edu.tr (H. Aydin)

**Table 1.** Chemical composition of 3003 aluminum alloy used in this study (wt.%)

Al	Si	Fe	Cu	Mn	Mg	Zn	Ti	Ga	V
Balance	0.201	0.665	0.053	1.082	0.127	0.014	0.021	0.011	0.018

fatigue data for the FSW joints of several aluminum alloys, especially the non-heat-treatable aluminum alloys, was relatively deficient. On the other hand, no published results have been presented on the fatigue behaviours of FS welded non-heat-treatable 3003-O aluminum alloys with particular attention to the variation of welding parameters. Among the Al-Mn system, also known as the 3XXX alloys series, the most widely used is the 3003 alloy. Al-Mn alloys have been used commercially since 1910. Owing to their good conformability, corrosion resistance, weldability, and allied reasonable mechanical resistance, they are becoming very interesting materials [22, 23].

The complicated microstructure around the weld zone mentioned above strongly govern the fatigue properties of FSW joints [7]. For the mechanical and fatigue properties of the FS welds, the welding parameters and the tools geometry represent critical issues [9, 24]. Therefore, the purpose of this research is to determine the effect of the welding parameters on the fatigue behaviour of single-sided FS butt-welded joints of the non-heat-treatable 3003-O aluminum alloy. Fatigue tests were conducted using the base material and the welds at a stress ratio  $R = -1$ . In addition, the microstructure and fractography of FS welds are studied.

## EXPERIMENTAL PROCEDURE

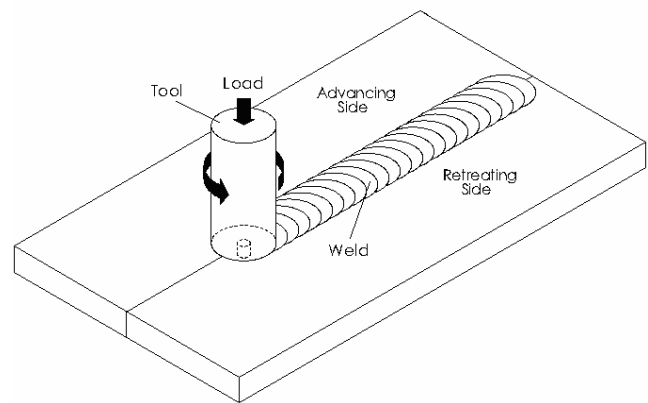
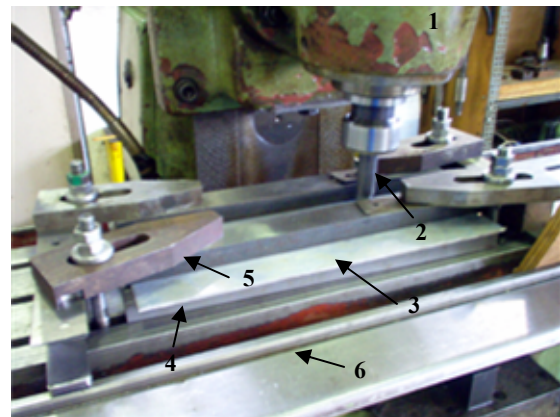
3003 rolled plates aluminum alloys in the O-temper state, whose chemical composition (wt.%) are listed in Table 1, was used as a workpiece material with the size of 100 mm × 360 mm and 3 mm thick. The material was produced as extruded flat profile. Tensile tests of the base material in Table 2 were carried out with the loading direction perpendicular to the rolling direction.

**Table 2.** Mechanical properties of 3003 aluminum alloy in the O-temper state

0.2 % Proof stress [MPa]	Tensile strength [MPa]	Elongation [%]
66	130	43.52

A schematic description of the FSW process can be seen in Fig. 1. The FSW does not produce a symmetric deformation with respect to the center line of the advancing tool [9, 25]. The advancing side (AS) of the weld is the side where the direction of rotation of the toolpiece is in the direction of travel of the toolpiece; on the retreating side (RS), the toolpiece rotation direction opposes the travel direction of the toolpiece [26] (Fig. 1). Design of the FSW machine fixture and backing is of utmost importance since the forces exerted by the tool are large [11]. Therefore, the initial joint configuration was obtained by securing the plates in position using mechanical clamps and a stainless steel backing plate was placed under the two butted base metal samples to be welded (Fig. 2). Then, the plates were friction-stir-welded

parallel to the rolling direction in the butt configuration using a vertical semiautomatic milling machine (Fig. 2). Single pass welding procedure was used to fabricate the joints and the axial force was kept constant at 30 kN. The employed rotating speeds of the tool were 1070, 1520 and 2140 rpm while the welding speeds were 40, 80 and 112 mm/min. The friction stir tool made of 1.2367 (X38CrMoV5-3) hardened steel was composed of a threaded probe, which was 2.9 mm long and of conical shape with a large diameter of 5 mm and small diameter of 4 mm, and a smooth shoulder whose diameter is 17 mm. The penetration depth was adapted to fully penetrated butt joint in a material of 3 mm thickness. The tool-to-workpiece angle was 2.5° from the vertical axis.

**Fig. 1.** Schematic representation of FSW process**Fig. 2.** FSW application on a conventional vertical milling machine: 1 – milling head, 2 – welding tool, 3 – aluminum plates, 4 – steel backing plate, 5 – clamping setup, 6 – machine table

The cross sections of the metallographic specimens were polished with alumina and diamond suspension, then etched by Keller's reagent with the following composition: 15 ml hydrochloric acid, 10 ml hydrofluoric acid, and 90 ml distilled water. The etching specimens were washed with absolute ethyl alcohol and then observed using an optical microscope.

Fatigue tests were performed in order to evaluate the fatigue behaviours of the FSWed 3003-O aluminum alloy joints obtained in the different welding conditions. The fatigue tests were carried out in a displacement-controlled uniaxial bending fatigue test machine at a frequency of 20 Hz at room temperature in laboratory air (Fig. 3).

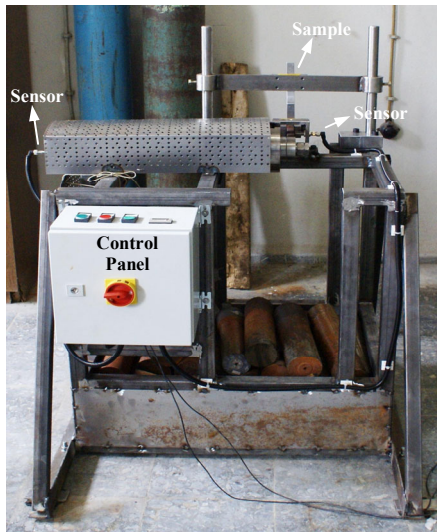


Fig. 3. Fatigue test machine used in this study

The fatigue test machine configuration can be also seen schematically in Fig. 4.

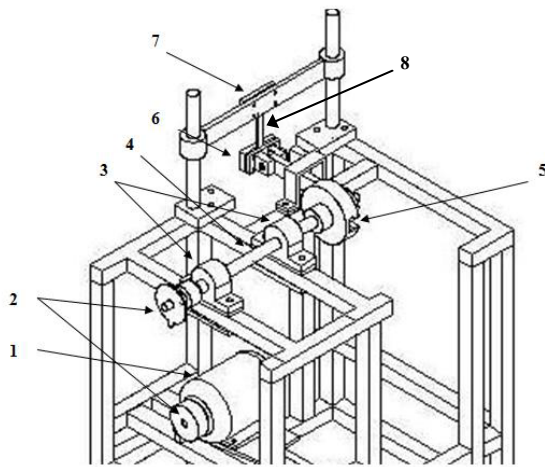


Fig. 4. Scheme of the fatigue test machine (1 – electric motor, 2 – belt-pulley mechanism, 3 – bearings, 4 – main shaft, 5 – amplitude (as displacement) control system (fly-wheel), 6 – steering joint, 7 – fixed joint, 8 – test sample)

The stress ratio  $R$  of the minimum stress to maximum stress was  $-1$ . The displacements used in the fatigue tests were selected as 2 mm, 3 mm, 4 mm, 5 mm and 6 mm. The displacement values in the fatigue tests corresponds to the calculated amplitude stress values of approximately 20 MPa, 30 MPa, 40 MPa, 50 MPa and 60 MPa. The fatigue data in this test are expressed as amplitude stress versus the corresponding life to failure (i.e. number of cycles) as represented in S–N diagrams. The fatigue specimens were sectioned in the perpendicular direction along the weld line. Prior to that, 60 mm at the beginning

and 30 mm at the end of the plate were removed to exclude possible deviation from steady state during start and stop. The weld was transverse to the stress axis in the S–N specimen (cross-weld). The dimensions of the fatigue specimens were 20 mm width, 200 mm length and 3 mm thickness. Prior to a fatigue tests, the surface of the gauge section was mechanically polished using a water proof silicon abrasive-paper of 1200 grade to prevent fatigue-cracking. All the fatigue tests were performed up to failure and some tests were conducted over  $10^7$  cycles. In addition, a scanning electron microscope was employed for the observation of the fracture surfaces of the fatigue specimens.

## RESULTS AND DISCUSSION

### Microstructure

The macroscopic views of the transverse cross sections of the joints near the weld zones can be seen in Fig. 5. No welding imperfections, such as voids, cracks or distortion, occurred in the bonding zone or on the back of the welding surface.

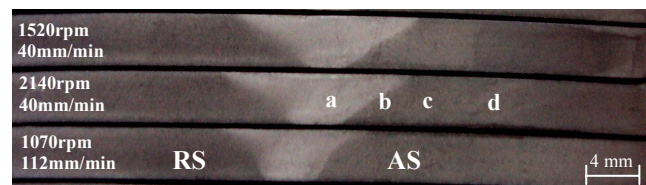
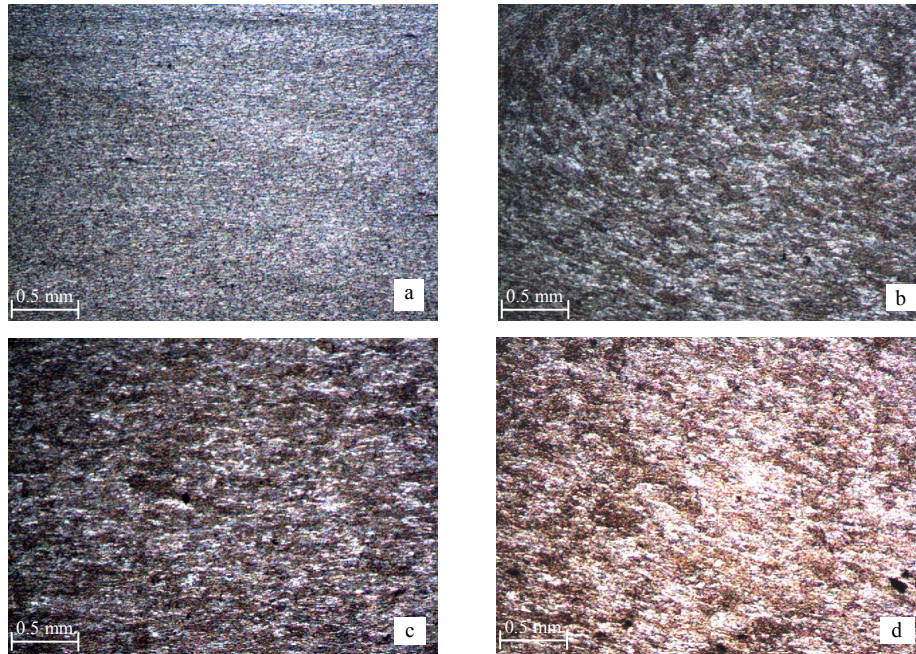


Fig. 5. A typical macroscopic images of the FSW 3003 joints

The distinct changes in microstructures of the weld zone are visible while testing the welded zones by means of optical microscope (Fig. 6). Fig. 6 illustrates details of the variation of the microstructure corresponding to regimes indicated by (a)–(d) in Fig. 5. There are several characteristic regions in the weld zone: base material, HAZ, TMAZ and stirred zone. At the centre is possible to identify the stirred zone (Fig. 6, a). In the stirred zone, a fine-grained equiaxial dynamic recrystallised microstructure can be seen, resulting from the high temperature and high rate of deformation in the stirred zone due to the pin's stirring [16]. The grain size in the stirred zone is obvious smaller than that of base material. Di et al. [21] reported that these fine-equiaxed recrystallized grains in the stirred zone could benefit to fatigue performance with longer initiating life of fatigue microcracks and higher fatigue crack growth resistance if fatigue crack was produced in the stirred zone. In addition, Fig. 7 shows optical micrographs of the grain structure in the stirred zone as a function of welding parameters. It is evident that the welding parameters affect the grain size in the stirred zone of weld. An increase in rotation speed and a decrease in welding speed decrease the grain size in the stirred zone due to the higher heat input for dynamic recrystallised microstructure. The TMAZ microstructure, where there is less heat and deformation compared to the stirred zone, characterized by a highly deformed structure near the stirred zone (Fig. 6, b, and Fig. 8). After the TMAZ appears the HAZ which experiences only a thermal cycle, but the plastic deformation in the HAZ is absent or

insufficient to modify the initial grain structure (Fig. 6, c). In addition, the microstructure of the base material can be seen in Fig. 6, d. The base material microstructure reveals the elongated grains belonging to the rolling operations. The transition zones from the stirred zone to TMAZ of the joints are also presented in Fig. 8. The AS is characterized by a typically distinct boundary between the stirred zone and the TMAZ (Fig. 8, a, b, c). On the other hand, the

boundary between the stirred zone and the TMAZ in the RS is rather unclear (Fig. 8, d, e, f). On the other hand, the typical ‘kissing bond’ defects were detected from the weld top to bottom across the whole section of all 3003-O FS weld zones at the RS (Fig. 9). Sato et al. [27, 28] have been reported that the particles in the ‘kissing bond’ region were  $Al_2O_3$  oxide.



**Fig. 6.** Microstructures of FSW joint (2140 rpm–40 mm/min) of 3003 Aluminum alloy: a – the stirred zone; b – TMAZ at the AS; c – HAZ at the AS; d – the base material

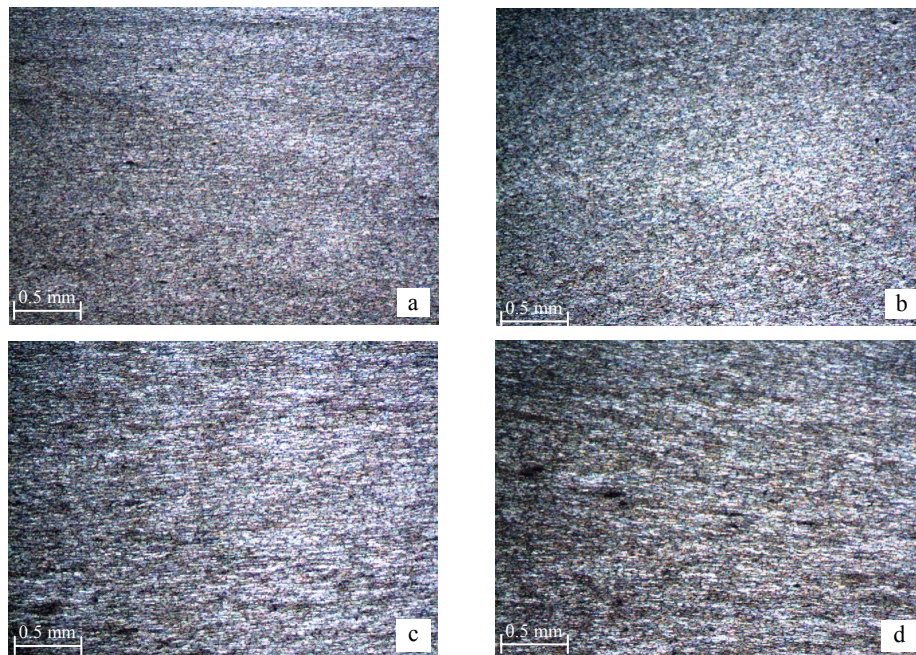


**Fig. 7.** Optical micrographs showing the grain structure in the stirred zone as a function of welding parameters: a – 2140 rpm–40 mm/min; b – 1520 rpm–80 mm/min; c – 1070 rpm–80 mm/min; (d) 1070 rpm–112 mm/min

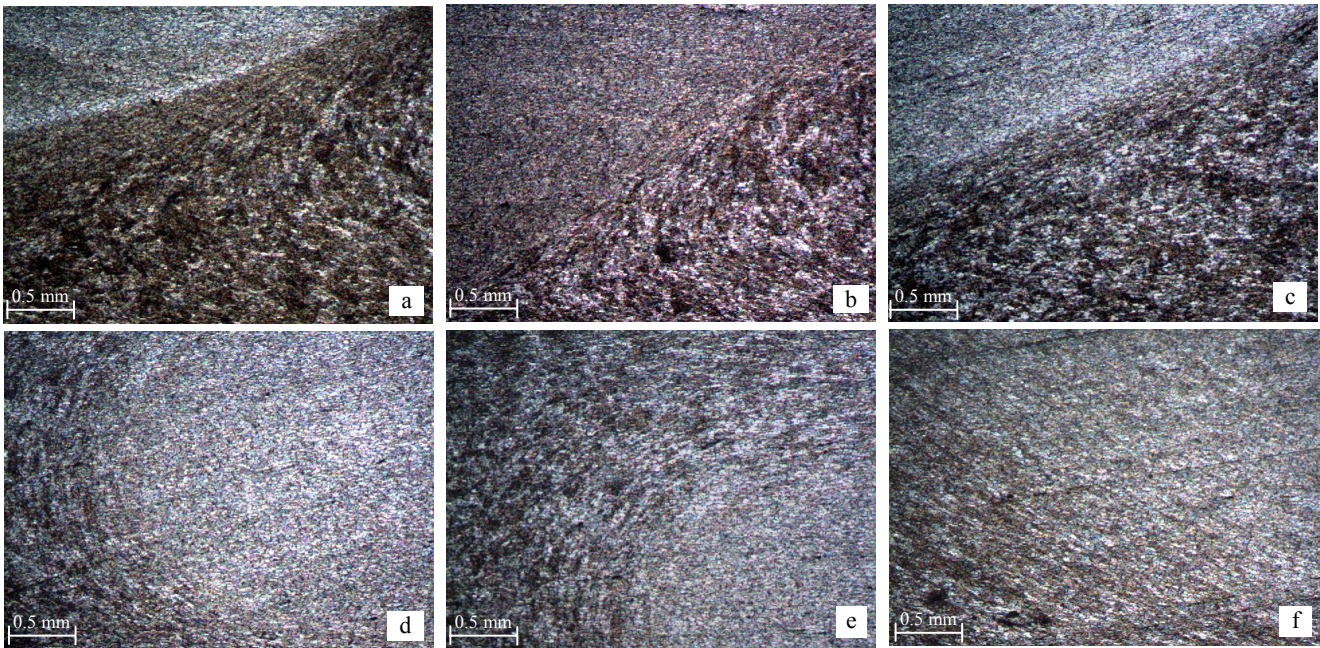


**Fig. 8.** Optical micrographs of the transition zones from the stirred zone to TMAZ (a, b, c) in the AS and (d, e, f) in the RS: a, d – 2140 rpm–40 mm/min; b, e – 2140 rpm–80 mm/min; c, f – 1520 rpm–80 mm/min

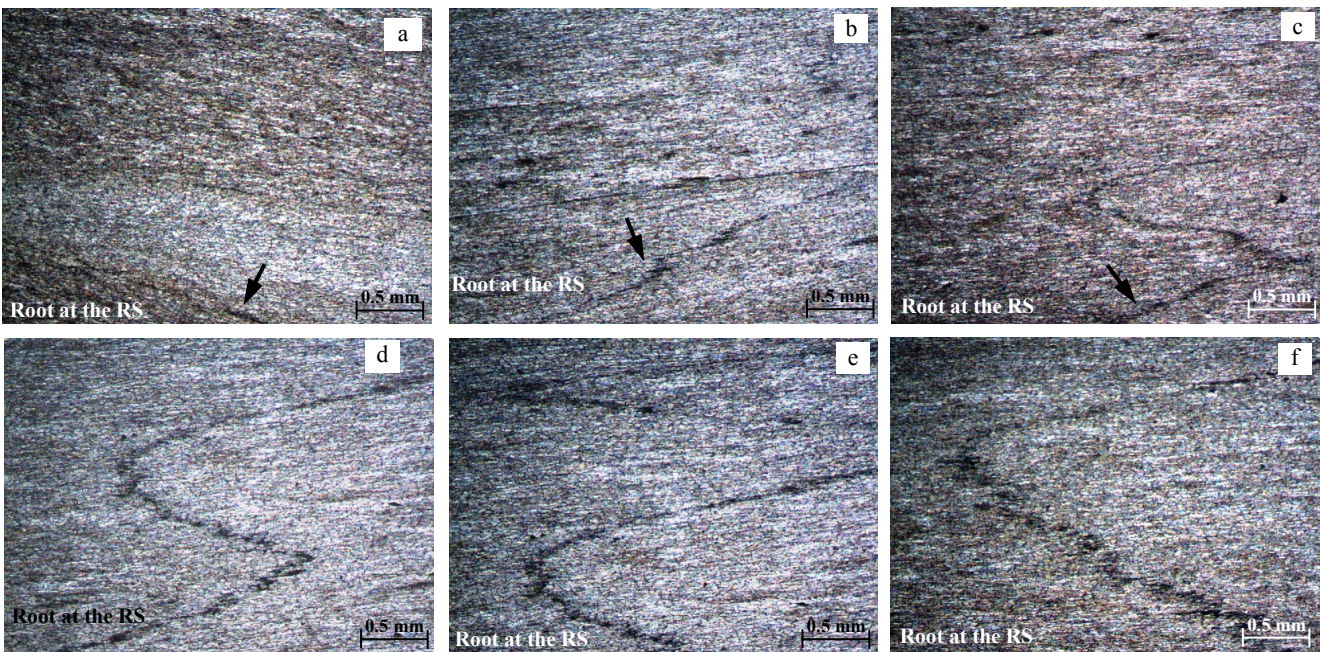


**Fig. 9.** The typical “kissing bond” defects in the weld zone at the RS across the section of 3003-O FS welds: a – 2140 rpm–40 mm/min; b – 1520 rpm–40 mm/min; c – 1070 rpm–40 mm/min; d – 2140 rpm–80 mm/min; e – 1520 rpm–80 mm/min; f – 1070 rpm–80 mm/min

### Fatigue behaviour

The comparison of fatigue S–N curves for 3003-O FS welds in different welding conditions and base material given in Figs. 10–15 indicated by the stress amplitude versus the number of cycles to failure. The curves in Figs. 10–15 show a classical behaviour revealing a trend of increasing fatigue life with decreasing cyclic stress amplitude. The points with arrows may have higher values for the welds as they did not fail in the test. There are major differences in fatigue behaviours between the FSW

specimens in different welding conditions. In addition, from the following fatigue test results it can be seen that the fatigue lives of FS welds are lower than those of the base material in 3003-O. Generally, FS material exhibits lower strength and ductility properties than the base material [4]. Cavaliere and Panella [9] also reported that FSW joints could offer fatigue limits lower than their corresponding base materials, but these limits are extremely higher if compared with those consequent to traditional fusion welds.

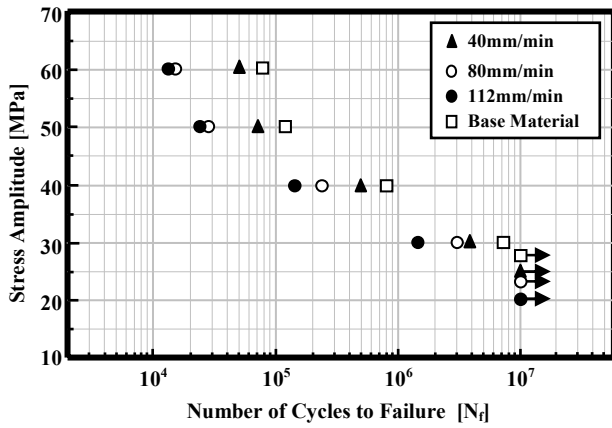


Fig. 10. S–N curves of the FSW joints in different welding speeds at 2140 rpm

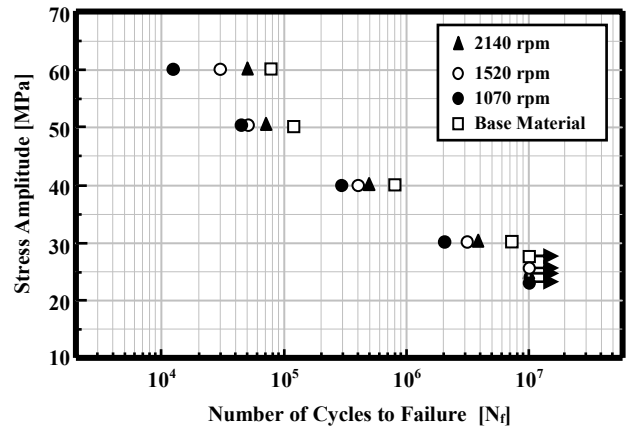


Fig. 13. S–N curves of the FSW joints in different rotation speeds at the welding speed of 40 mm/min

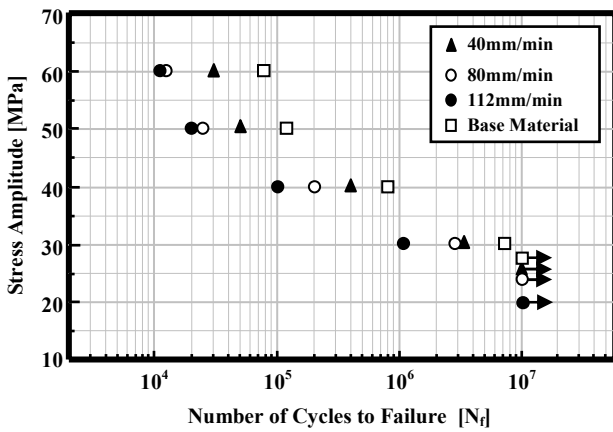


Fig. 11. S–N curves of the FSW joints in different welding speeds at 1520 rpm

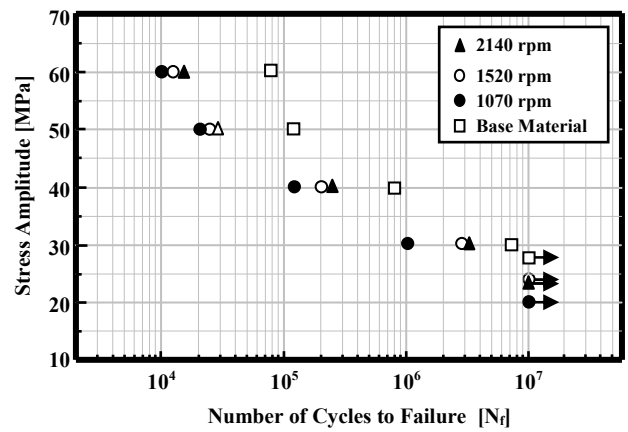


Fig. 14. S–N curves of the FSW joints in different rotation speeds at the welding speed of 80 mm/min

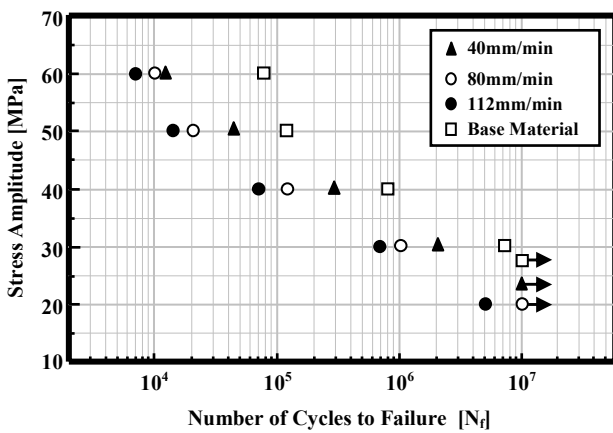


Fig. 12. S–N curves of the FSW joints in different welding speeds at 1070 rpm

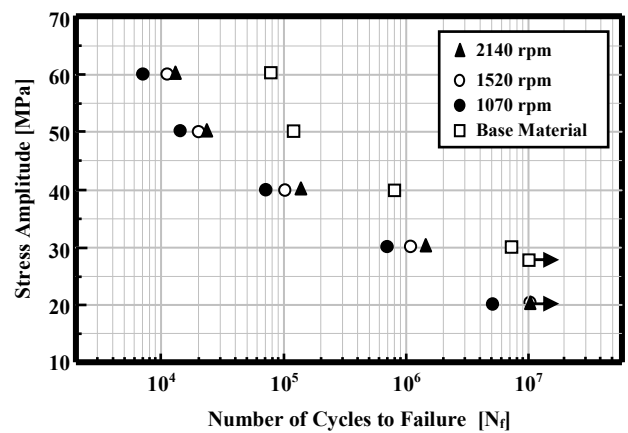


Fig. 15. S–N curves of the FSW joints in different rotation speeds at the welding speed of 112 mm/min

The influence of welding speed at a constant rotational speed on the fatigue behaviours of the FS welds is illustrated in Figs. 10–12, while Figs. 13–15 show the influence of rotational speed at a constant welding speed. In the FS welds of 3003-O aluminum alloys, it was confirmed that the welding parameters (welding speed and rotation speed) exert significantly influence on the fatigue behaviour. The test results show that the fatigue performance of the FSW joints does decline with increased welding speed and decreased rotational speed in the tested interval. The fatigue behaviours of FS welds with a lower welding speed at a higher rotation speed are entirely better than those of FS welds with a higher welding speed at a lower rotation speed. As can be seen in Figs. 10–15, the fatigue lives of FS welds with the welding speed of 40 mm/min at different rotating speeds are about 2–3 times longer than those of FS welds with the welding speeds of 80 mm/min and 112 mm/min at different rotating speeds at a fixed stress amplitude under the stress ratio  $R = -1$ . That means that lower welding speeds during FSW process can effectively lengthen the fatigue lives of FS welded non-heat-treatable 3003-O aluminum alloy. In addition, from Figs. 10–15, it can be said that the welding speed was more effective on the fatigue behaviours of the FSWed 3003-O joints than the rotation speed. Cavaliere and Panella [9] also reported that the fatigue strength of the most common alloys decreases as the ratio welding speed/rotating speed is higher. Furthermore, Ericsson and Sandström [11] stated that the low welding speed gave the best results for the fatigue performance of FS welded 6082 aluminum alloy. In addition, Ericsson and Sandström [11] reported that with a lower welding speed, the amount of heat supplied to the weld region was greater and therefore the metal flow and creation of the weld might have been more effective. These could explain the

relatively high fatigue behaviours of the FS welds with a lower welding speed and a higher rotational speed.

Fatigue test results show that the fatigue fractures of all FSW joints occurred at the between TMAZ and the stirred zone at the RS. For FS welds, fracture during fatigue loading propagated in the root site of the welds, which usually occurs due to low heat input or improper tool orientation and ‘kissing bond’ in the root at the RS (Fig. 9). The features of the fatigue fracture surfaces of the FSW joints tested at stress amplitude of 40 MPa were examined by using SEM. The typical fracture surfaces of FSWed 3003-O aluminum alloys, after the fatigue tests are presented in Fig. 16. All fracture appearances possess plastic tearing mark. The FS welds in different welding conditions exhibit almost similar crack propagation behaviours. The fractures of the fatigue specimens exhibited regions of crack initiation, stable crack growth and overload. Stable crack growth in the fatigue specimens during fatigue test occurred by mechanisms that resulted in the formation and presence of striation-like features. Fatigue striations in all fatigue specimens are visible on the surfaces of the fatigue zones (Fig. 16). The fatigue striation in the fatigue test specimens revealed pockets of heterogeneously distributed striation-like features indicative of localized microplastic deformation. The ductile fracture features in the fatigue specimens are more obvious. With the welding speed at a higher rotating speed increases the ductile fracture feature is more apparent as shown in Fig. 17. In the fracture surfaces of the weld with the welding speed of 112 mm/min at 2140 rpm, striation-like features and the presence of local ductility with small dimples and voids in the zones surrounding the striations were observed in the region of stable crack growth (Fig. 17, c).

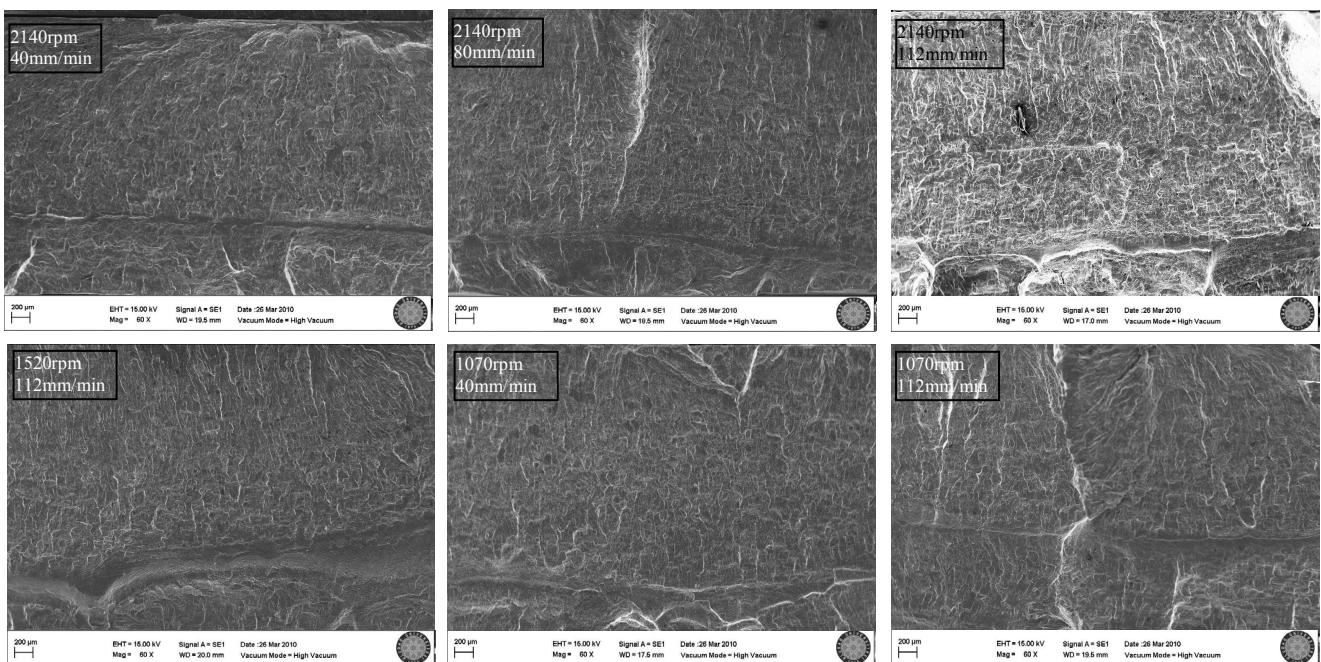
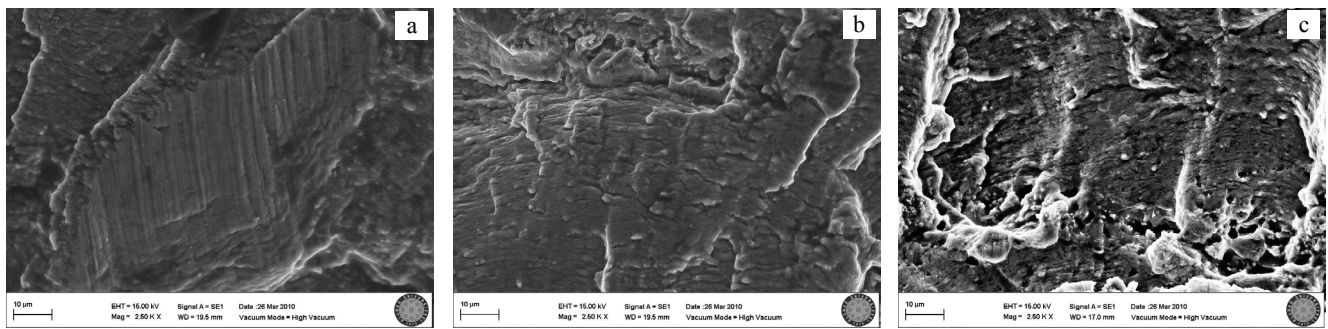


Fig. 16. SEM images of fatigue fracture surfaces of FS welded joints



**Fig. 17.** SEM images of fatigue fracture surfaces of FS welded joints with the welding speeds of 40 mm/min (a), 80 mm/min (b) and 112 mm/min (c) at the rotation speed of 2140 rpm

## CONCLUSIONS

The fatigue behaviours of the FS welded joints of the non-heat-treatable 3003-O aluminum alloy in different welding conditions were investigated at the same experimental condition. The following conclusions were drawn:

All FSW welds in different welding conditions of 3003-O aluminum alloy exhibit lower fatigue life than the base material.

Fatigue behaviours of the FS welds of the non-heat-treatable 3003-O aluminum alloy are dependent of welding parameters (welding speed and rotational speed). The lower welding speed and higher rotational speed are beneficial for the fatigue performance of 3003-O aluminum alloy. The fatigue lifes of FS welds with the welding speed of 40 mm/min at different rotating speeds are about 2–3 times longer than those of FS welds with the welding speeds of 80 mm/min and 112 mm/min at different rotating speeds at a fixed stress amplitude under the stress ratio  $R = -1$ . This improvement in the fatigue life of the friction stir welds with a lower welding speed and a higher rotational speed can be associated with the increased amount of heat supplied to the weld per unit length. Furthermore, the welding speed was more effective on the fatigue behaviours of the FSWed 3003-O joints than the rotation speed.

The location of fatigue fracture is not dependent on welding parameters. For all the fractured specimens, cracks initiated from the root part at the between TMAZ and the stirred zone at the retreating side of the FS 3003-O welds. This can be explained by ‘kissing bond’ defect in the root side of the welds at the RS.

These results obtained in this study can generate a general prediction for the fatigue behaviours of the other non-heat-treatable aluminum alloys welded by FSW technique.

## REFERENCES

1. **Aydın, H., Demirci, A. H.** Wear Behaviour of Aged Al-Cu-Mg Alloys Sliding Against C45 Steel and SiC Abrasive Paper *Materialprüfung* 49 (5) 2007: pp. 253–257.
2. **Zhou, C., Yang, X., Luan, G.** Fatigue Properties of Friction Stir Welds in Al 5083 Alloy *Scripta Materialia* 53 2005: pp. 1187–1191.
3. **Zhou, C., Yang, X., Luan, G.** Investigation of Microstructures and Fatigue Properties of Friction Stir Welded Al-Mg Alloy *Materials Chemistry and Physics* 98 2006: pp. 285–290.
4. **Moreira, P. M. G. P., Jesus, A. M. P. de, Ribeiro, A. S., Castro, P. M. S. T. de.** Fatigue Crack Growth in Friction Stir Welds of 6082-T6 and 6061-T6 Aluminium Alloys: A comparison *Theoretical and Applied Fracture Mechanics* 50 2008: pp. 81–91.
5. **Czechowski, M.** Low-cycle Fatigue of Friction Stir Welded Al-Mg Alloys *Journal of Materials Processing Technology* 164–165 2005: pp. 1001–1006.
6. **Thomas, W. M., Nicholas, E. D., Needham, J. C., Church, M. G., Templesmith, P., Dawes, C. J.** GB Patent Application, No. 9125978.9, 1991.
7. **Uematsu, Y., Tokaji, K., Shibata, H., Tozaki, Y., Ohmune, T.** Fatigue Behaviour of Friction Stir Welds without neither Welding Flash Nor Flaw in Several Aluminium Alloys *International Journal of Fatigue* 31 2009: pp. 1443–1453.
8. **Aydın, H., Bayram, A., Uğuz, A., Akay, S. K.** Tensile Properties of Friction Stir Welded Joints of 2024 Aluminum Alloys in Different Heat-treated State *Materials Design* 30 (6) 2009: pp. 2211–2221.
9. **Cavaliere, P., Panella, F.** Effect of Tool Position on The Fatigue Properties of Dissimilar 2024-7075 Sheets Joined by Friction Stir Welding *Journal of Materials Processing Technology* 206 2008: pp. 249–255.
10. **Lomolino, S., Tovo, R., dos Santos, J.** On The Fatigue Behaviour and Design Curves of Friction Stir Butt-welded Al Alloys *International Journal of Fatigue* 27 2005: pp. 305–316.
11. **Ericsson, M., Sandström, R.** Influence of Welding Speed on The Fatigue of Friction Stir Welds, and Comparison with MIG and TIG *International Journal of Fatigue* 25 2003: pp. 1379–1387.
12. **Dickerson, T. L., Przydatek, J.** Fatigue of Friction Stir Welds in Aluminium Alloys that Contain Root Flaws *International Journal of Fatigue* 25 2003: pp. 1399–1409.
13. **Thomas, W. M., Dawes, C., Gittos, M., Andrews, R.** Friction Stir – Where We Are and Where We’re Going *TWI Bulletin* 39 (3) 1998.
14. **Aydın, H., Bayram, A., Durgun, I.** The Effect of Post-weld Heat Treatment on The Mechanical Properties of 2024-T4 Friction Stir-welded Joints *Materials Design* 31 (5) 2010: pp. 2568–2577.
15. **Mahoney, M. W., Rhodes, C. G., Flintoff, J. G., Bingel, W. H., Spurling, R. A.** Properties of Friction-stir-welded 7075 T651 Aluminum *Metallurgical and Materials Transactions A* 29 (7) 1998: pp. 1955–1964.
16. **Jata, K. V., Semiatin, S. L.** Continuous Dynamic Recrystallization During Friction Stir Welding of High Strength Aluminum Alloys *Scripta Materialia* 43 (8) 2000: pp. 743–749.

17. **Flores, O. V., Kennedy, C., Murr, L. E., Brown, D., Pappu, S., Nowak, B. M., et al.** Microstructural Issues in a Friction-stir-welded Aluminum Alloy *Scripta Materialia* 38 (5) 1998: pp. 703–708.
18. **Cavaliere, P.** Effect of Friction Stir Processing on the Fatigue Properties of a Zr-modified 2014 Aluminium Alloy *Materials Characterisation* 57 2006: pp. 100–104.
19. **Salem, H. G., Reynolds, A. P., Lyons, J. S.** Microstructure and Retention of Superplasticity of Friction Stir Welded Superplastic 2095 Sheet *Scripta Materialia* 46 2002: pp. 337–342.
20. **Charit, I., Mishra, R. S., Mahoney, M. W.** Multi-sheet Structures in 7475 Aluminum by Friction-stir Welding in Concert with Post-weld Superplastic Forming *Scripta Materialia* 47 2002: pp. 631–636.
21. **Di, S., Yang, X., Luan, G., Jian, B.** Comparative Study on Fatigue Properties Between AA2024-T4 Friction Stir Welds and Base Materials *Materials Science and Engineering A* 435–436 2006: pp. 389–395.
22. **Martins, J. P., Carvalho, A. L. M., Padilha, A. F.** Microstructure and Texture Assessment of Al-Mn-Fe-Si (3003) Aluminum Alloy Produced by Continuous and Semicontinuous Casting Processes *Journal of Materials Science* 44 2009: pp. 2966–2976.
23. **Mondolfo, L. F.** In: Bros P, Lane MC (eds) Manganese in Aluminum Alloys. The Manganese Centre, Nevilly sur Seine, 1977: p. 118.
24. **James, M. N., Bradley, G. R., Lombard, H., Hattingh, D. G.** The Relationship Between Process Mechanisms and Crack Paths in Friction Stir Welded 5083-H321 and 5383-H321 Aluminium Alloys *Fatigue & Fracture of Engineering Materials & Structures* 28 2005: pp. 245–256.
25. **Buffa, G., Donati, L., Fratini, L., Tomesani, L.** Solid State Bonding in Extrusion and FSW: Process Mechanics and Analogies *Journal of Materials Processing Technology* 177 2006: pp. 344–347.
26. **Jariyaboon, M., Davenport, A. J., Ambat, R., Connolly, B. J., Williams, S. W., Price, D. A.** The Effect of Welding Parameters on The Corrosion Behaviour of Friction Stir Welded AA2024–T351 *Corrosion Science* 49 2005: pp. 877–909.
27. **Sato, Y. S., Takauchi, H., Park, S. H. C., Kokawa, H.** Characteristics of The Kissing-bond in Friction Stir Welded Al Alloy 1050 *Materials Science and Engineering A* 405 2005: pp. 333–338.
28. **Sato, Y. S., Yamashita, F., Sugiura, Y., Park, S. H. C., Kokawa, H.** FIB-assisted TEM Study of an Oxide Array in The Root of a Friction Stir Welded Aluminium Alloy *Scripta Materialia* 50 2004: pp. 365–369.

